

Steric Effect Determines the Formation of Lactam–Lactam Dimers or Amide C=O⋯NH (Lactam) Chain Motifs in *N*-Phenyl-2-hydroxynicotinilides

H. Liu,[#] X. Yang,[#] S. Cao, F. Yu,^{*} S. Long,^{*} J. Chen, M. Zhang, S. Parkin, T. Li, and Z. YangCite This: *Cryst. Growth Des.* 2020, 20, 4346–4357

Read Online

ACCESS |



Metrics & More

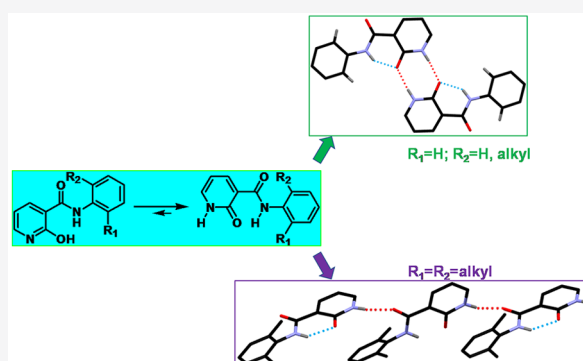


Article Recommendations



Supporting Information

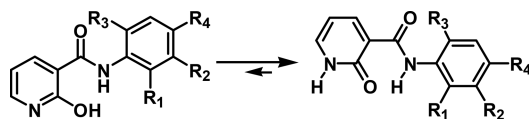
ABSTRACT: A series of *N*-phenyl-2-hydroxynicotinilides (PHNAs) have been synthesized, and their crystal structures have been investigated. The identity of these compounds is revealed to be the tautomer of PHNAs, i.e., 2-oxo-1,2-dihydropyridine-3-carboxylic acid phenylamides, compounds with both amide and lactam functionalities. Among these compounds, those with no or negligible steric hindrance take a near planar conformation and form lactam–lactam dimers, not the widely observed amide NH⋯O=C hydrogen bond chains, while those with steric hindrance take a twisted conformation and form an amide NH⋯O=C (lactam) hydrogen bond. A succinct theoretic study combining conformational analysis and molecular electrostatic potential surfaces (MEPS) survey provided a reasonable explanation of the formation of these two different hydrogen bond motifs.



1. INTRODUCTION

In this work, we investigate the solid-state structural properties of a series of *N*-phenyl-2-hydroxynicotinilides (PHNAs) (Scheme 1), compounds with an interesting structure and some with potent anti-inflammatory activity.^{1–3}

Scheme 1. Tautomerization in PHNAs



By name, PHNAs are amide compounds from the condensation between 2-hydroxynicotinic acid and aniline(s). We previously investigated the crystal structures of 2-, 4-, and 6-hydroxynicotinic acid and found out that these compounds actually exist in their tautomers, i.e., 2-oxo-1,2-dihydropyridine-3-carboxylic acid, 4-oxo-1,4-dihydropyridine-3-carboxylic acid, and 6-oxo-1,6-dihydropyridine-3-carboxylic acid, respectively.^{4–6} 5-Hydroxynicotinic acid has also been studied. In the 5-position, the hydroxyl group does not have a vinylogous relationship with the nicotinic N. The tautomer would have to be a zwitterion with the O atom chiefly bearing the negative charge and the NH function bearing most of the partial positive charge. Nevertheless, a series of crystals have been produced⁷ (Scheme 2).

Will the same tautomerization be observed for PHNAs? If so, the compounds would have two sets of amides, one

conventional (open chain) and the other lactam. For amides from primary amines, C=O and NH are in general trans (manifested by peptides and the compounds in this work), while for lactams, C=O and NH are cis due to the ring formation. For amides, the normally observed hydrogen bond motif is C=O⋯HN chains (catemer), as observed in the sheet structure in peptides, or long-range C=O⋯HN in helices.^{8–10} The situation for terminal -CONH₂- such as that in carbamazepine could be complicated due to the presence of two H's.^{11,12} For lactam, the molecules form R₂²(8) homodimers most of the time with no other interference¹³ (Scheme 3).

If the molecules we synthesized actually exist as the lactam tautomer, then the presence of both amide and lactam, β to each other, in an end-to-end fashion, makes the situation complicated. Will the catemer motif prevail, or the dimer predominate? What role will steric hindrance play? The answers are revealed in this work, through a combination of experimental and theoretical approaches.

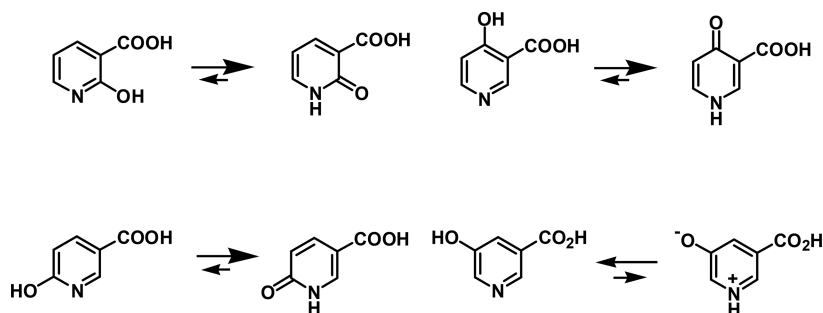
Received: January 7, 2020

Revised: April 27, 2020

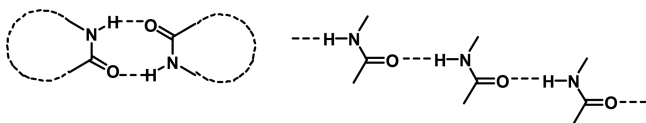
Published: April 29, 2020



Scheme 2. Tautomerization in HNAs



Scheme 3. Lactam–Lactam Dimer and Catemer in Lactam and Amide



2. EXPERIMENTAL SECTION

2.1. Materials. All chemicals were purchased from commercial sources: anilines were from Bide Pharmatech Ltd. (Shanghai, China); thionyl chloride, triethylamine, sulfuric acid and 2-chloronicotinic acid were from Aladdin Industrial Corporation; and solvents for crystal growth were from Sinopharm Chemical Reagent Co., Ltd. (Shanghai, China) and were used as received.

2.2. Synthesis. In this study, 12 PHNAs, grouped into two series (1 and 2), one with no or negligible steric hindrance (compounds 1–8) and the other with various degrees of steric repulsion (compounds 9–12), have been synthesized,^{1,14,15} and their crystal structures have been investigated (Figure 1). (For detailed synthesis procedure and characterization, see Supporting Information.)

2.3. Crystal Growth and Structure Determination. Crystals of each compound were harvested from a suitable solvent for that compound through slow evaporation.¹⁶ The crystal structures of PHNAs were determined by single-crystal X-ray diffraction^{17–20} (for details, see Supporting Information). The crystallographic data of compounds 1–8 are listed in Table 1.

Compounds 1–8 (Figure 1) are either unsubstituted or monosubstituted at one of the *ortho* positions of the aniline ring, thus with no or negligible steric hindrance. The molecules take a near planar conformation as indicated by the dihedral angle between the two rings in each molecule (Table 2). As a result, the lactam–lactam dimers, not the normal amide NH...O=C hydrogen bond chains, are observed in the crystal structures.

3. RESULTS AND DISCUSSION

3.1. Structural Properties. *Compound 1.* The molecule is nearly flat with a dihedral angle between the two aromatic rings of 9.85(6)°, likely due to being free of steric hindrance. The molecules form dimers based on the lactam–lactam R₂²(8)²¹ hydrogen bonding motif. In addition, the lactam C=O forms an intramolecular hydrogen bond with the NH from the amide, in a bifurcating hydrogen bonding fashion, while the

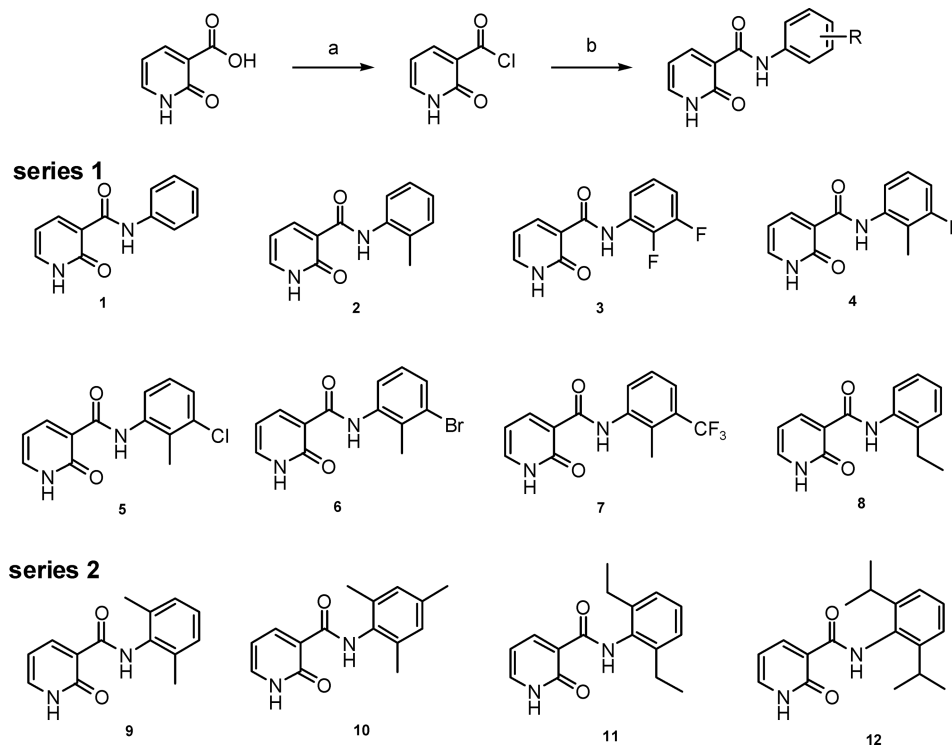


Figure 1. Synthesis of PHNAs. Reagents and condition: (a) SOCl₂/CH₂Cl₂, reflux 3 h; (b) aniline/CH₂Cl₂, reflux 3 h.

Table 1. Crystallographic Data of Compounds 1–8

	1	2	3	4	5	6	7	8
formula	C ₁₂ H ₁₀ N ₂ O ₂	C ₁₃ H ₁₂ N ₂ O ₂	C ₁₂ H ₈ F ₂ N ₂ O ₂	C ₁₃ H ₁₁ FN ₂ O ₂	C ₁₃ H ₁₁ ClN ₂ O ₂	C ₁₃ H ₁₁ BrN ₂ O ₂	C ₁₄ H ₁₁ F ₃ N ₂ O ₂	C ₁₄ H ₁₄ N ₂ O ₂
formula weight	214.22	228.25	250.20	246.24	262.69	307.15	296.25	242.27
crystal size	0.50 × 0.20 × 0.20	0.40 × 0.10 × 0.05	0.40 × 0.20 × 0.10	0.40 × 0.30 × 0.02	0.20 × 0.10 × 0.03	0.30 × 0.10 × 0.04	0.30 × 0.10 × 0.05	0.30 × 0.20 × 0.10
crystal system	monoclinic	monoclinic	monoclinic	triclinic	triclinic	triclinic	monoclinic	monoclinic
space group	P2 ₁ /c	P2 ₁ /c	P2 ₁ /c	P $\bar{1}$	P $\bar{1}$	P $\bar{1}$	P2 ₁ /c	P2 ₁ /c
a/Å	5.3686(3)	4.6946(10)	7.26050(10)	7.423(11)	7.1514(2)	7.164(1)	7.2021(3)	8.1790(3)
b/Å	20.0938(10)	15.0107(3)	7.27930(10)	7.155(1)	7.5805(2)	7.715(1)	23.0479(9)	9.3125(3)
c/Å	9.9143(6)	15.4831(3)	19.8474(4)	10.138(2)	10.3268(3)	10.446(2)	7.4429(3)	16.4409(6)
α /°	90	90	90	90.12(1)	87.8186(14)	88.23(1)	90	90
β /°	103.988(5)	98.3020(8)	95.4271(9)	92.70(1)	89.5131(14)	89.18(1)	90.2459(18)	93.853(3)
γ /°	90	90	90	89.28(1)	89.2959(13)	89.68(1)	90	90
Z, Z'	4, 1	4, 1	4, 1	2, 1	2, 1	2, 1	4, 1	4, 1
V/Å ³	1037.79(10)	1079.65(4)	1044.26(3)	537.80(15)	559.36(3)	577.01(16)	1235.46(9)	1249.43(7)
D _{cal} /g cm ⁻³	1.371	1.404	1.591	1.521	1.56	1.768	1.593	1.288
T/K	293(2)	90(2)	90(2)	90(2)	90(2)	90(2)	90(2)	293(2)
Abs coeff (mm ⁻¹)	0.786	0.097	0.134	0.116	0.336	3.556	0.138	0.711
F(000)	448	480	512	256	272	308	608	512
θ range (deg)	4.401–71.965	1.90–27.50	1.46–27.47	2.01–27.49	1.66–27.50	1.95–27.47	1.77–27.48	5.393–66.666
limiting indices	-6 ≤ h ≤ 5	-6 ≤ h ≤ 6	-9 ≤ h ≤ 9	-9 ≤ h ≤ 9	-9 ≤ h ≤ 9	-9 ≤ h ≤ 9	-9 ≤ h ≤ 9	-9 ≤ h ≤ 9
	-24 ≤ k ≤ 18	-19 ≤ k ≤ 19	-9 ≤ k ≤ 9	-9 ≤ k ≤ 9	-9 ≤ k ≤ 9	-10 ≤ k ≤ 10	-29 ≤ k ≤ 29	-11 ≤ k ≤ 11
	-12 ≤ l ≤ 11	-20 ≤ l ≤ 20	-25 ≤ l ≤ 25	-13 ≤ l ≤ 13	-13 ≤ l ≤ 13	-13 ≤ l ≤ 13	-9 ≤ l ≤ 9	-19 ≤ l ≤ 19
completeness to 2 θ (%)	99.00	99.90	99.90	99.70	99.90	99.70	99.90	100
unique reflections	1582	1851	1736	1986	1811	2273	1694	1677
R ₁ [<i>I</i> > 2 σ (<i>I</i>)]	0.048	0.0441	0.0478	0.041	0.0446	0.0313	0.0477	0.0465
wR ₂ (all data)	0.1461	0.1215	0.1417	0.1122	0.1123	0.072	0.1287	0.1518
CCDC accession code	1975829	1975832	1975833	1975834	WEPCAW	YAXJOY	1975835	1975838

Table 2. Values of the Dihedral Angle, τ , of the Molecules in the Crystal Structures of Compounds 1–8

1	2	3	4	5	6	7	8
9.85(6) $^\circ$	6.35 (4) $^\circ$	2.54 (5) $^\circ$	6.03(4) $^\circ$	7.58(6) $^\circ$	8.38(7) $^\circ$	7.19 (7) $^\circ$	15.21 (6)

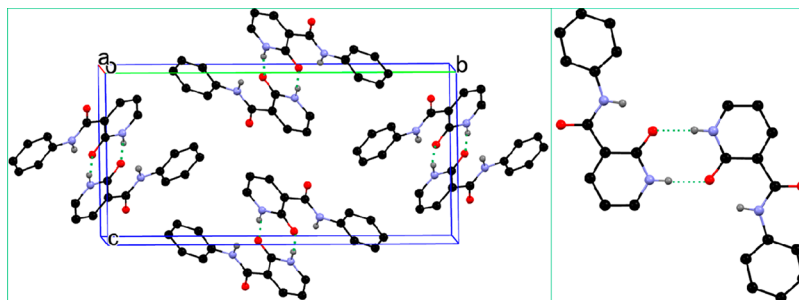


Figure 2. Crystal packing of compound 1 and the lactam–lactam synthon. For clarity, H's not participating in hydrogen bonds are omitted.

C=O from the amide is idle (Figure 2). The intermolecular hydrogen bond has a hydrogen bond length of 1.916 Å and a hydrogen bond angle of 170.02 $^\circ$, while the intramolecular hydrogen bond has parameters of 1.884 Å and 145.92 $^\circ$.

Compound 2. Although one of the H's at the *ortho* positions of aniline is replaced with a methyl group, steric repulsion between CH₃ and C=O of the amide can be avoided by rotating along the N–C (aniline) bond. Like compound 1, the molecule takes a planar conformation with the same dihedral angle being 6.35(4) $^\circ$. As a result, molecules of compound 2 behave exactly like those of compound 1, forming dimers based on the lactam–lactam R₂²(8) hydrogen bonds. The lactam C=O also forms a bifurcated intramolecular hydrogen bond with NH from the amide (S6) (Figure 3). The hydrogen bond parameters of inter- and intramolecular hydrogen bonds are as follows: 1.886 Å, 172.38 $^\circ$ and 1.895 Å, 144.59 $^\circ$, respectively.

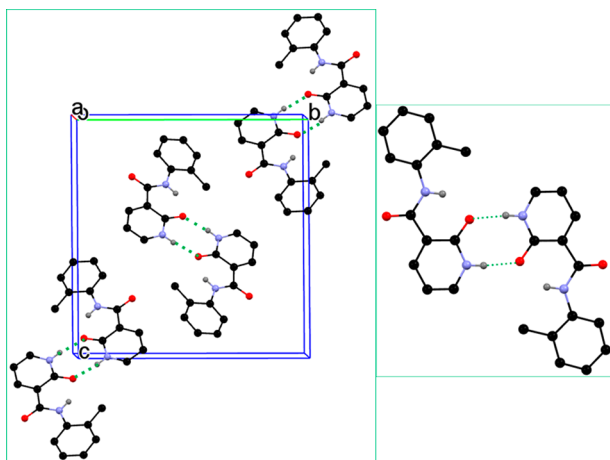


Figure 3. Crystal packing of compound 2 and the lactam–lactam synthon. For clarity, H's not participating in hydrogen bonds are omitted.

Compound 3. The two H's at the 2 and 3 positions of the aniline are replaced with two fluorines (F). As known, F is similar to H in size, but it is highly electronegative. In one of our previous studies, we successfully applied fluorine substitution on the aniline to force the planar conformation in 2-PNAs.²² Here, the same effect is observed, as the difluoro substituted compound 3 has a nearly perfectly planar

conformation, as indicated by the dihedral angle of 2.54(5) $^\circ$. Not surprisingly, the hydrogen bonding patterns are the same as those in compounds 1 and 2, i.e., forming intermolecular dimers based on a lactam–lactam R₂²(8) hydrogen bonding motif (Figure 4). The corresponding hydrogen bond parameters are as follows: 1.917 Å, 167.90 $^\circ$ intermolecularly; and 1.906 Å, 141.38 $^\circ$ intramolecularly.

Compound 4. The two H's at the 2 and 3 positions are replaced by CH₃ and F respectively. The crystal structure is expected to take after that of compound 2, likely with a slightly flatter conformation. It turned out to be the case as the CH₃ is *cis* to amide NH, and the dihedral angle is 6.03 (4) $^\circ$, and lactam–lactam R₂²(8) dimers are observed (Figure 5). The hydrogen bond parameters are as the follows: intermolecular hydrogen bond: 1.925 Å and 166.95 $^\circ$, and intramolecular hydrogen bond: 1.900 Å and 143.36 $^\circ$.

Compound 5. Compound 5 is analogous to compound 4 as the F in 4 is replaced with Cl in 5. Cl has a larger size and less electronegativity with regard to F. Compound 5 is expected to behave similarly to compound 4, likely with a larger dihedral angle between the two aromatic rings. In practice, the molecule of compound 5 has an overall similar conformation as that of compound 4 molecule, with the dihedral angle being 7.58 (6) $^\circ$ (Figure 6). The hydrogen bonding patterns are the same with hydrogen bond parameters: 1.920 Å and 169.56 $^\circ$ for the intermolecular hydrogen bond, and 1.890 Å and 144.33 $^\circ$ for the intramolecular hydrogen bond.

Compound 6. Compound 6 is to compound 5 as compound 5 to compound 4. No obvious difference is observed except for the dihedral angle slightly higher at 8.38 (7) $^\circ$ (Figure 7). The hydrogen bond parameters are similar to those of compound 5: 1.913 Å and 171.16 $^\circ$ for intermolecular hydrogen bond, and 1.896 Å and 144.29 $^\circ$ for intramolecular hydrogen bond.

Compound 7. Compound 7 is a bioisostere of compounds 5 and 6. The strategy of CH₃(CF₃)/Cl exchange is widely applied in medicinal chemistry.^{23–25} Compound 7 behaves in the same manner as compounds 5 and 6 (Figure 8). Likely because the accumulative electronegativity of three F's is strong enough to rival that of Cl, the molecule is slightly flatter than that of compound 6. The hydrogen bond style is the same as the ones of the previous compounds and with similar hydrogen bond parameters: 1.917 Å and 168.21 $^\circ$ for intermolecular hydrogen bond, and 1.910 Å and 143.57 $^\circ$ for intramolecular hydrogen bond. Should CF₃ be replaced by

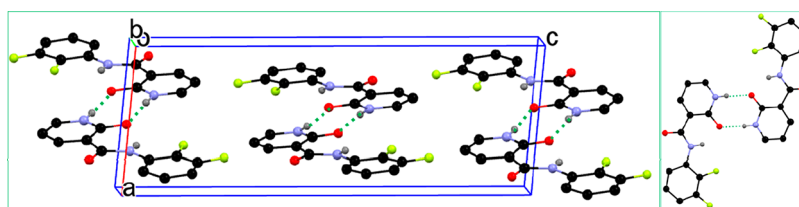


Figure 4. Crystal packing of compound 3 and the lactam–lactam synthon. For clarity, H's not participating in hydrogen bonds are omitted.

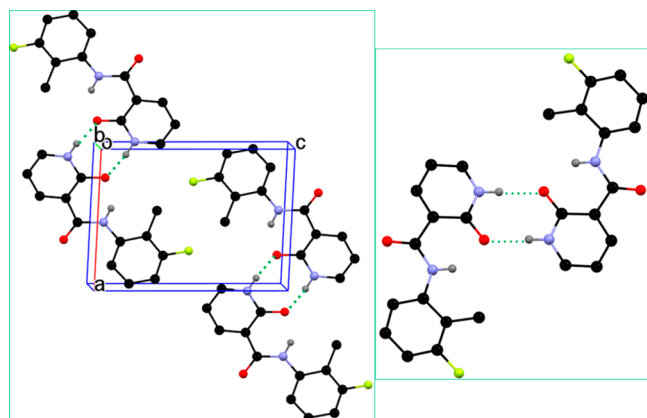


Figure 5. Crystal packing of compound 4 and the lactam–lactam synthon. For clarity, H's not participating in hydrogen bonds are omitted.

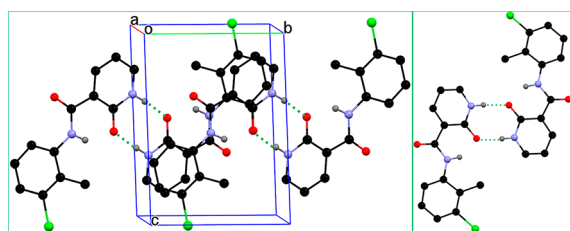


Figure 6. Crystal packing of compound 5 and the lactam–lactam synthon. For clarity, H's not participating in hydrogen bonds are omitted.

CH₃, the structure likely would be isostructural to compound 8.

Compound 8. In compound 8, an ethyl group is introduced at the ortho position of the aniline. Yet, since the steric hindrance between CH₃CH₂ and C=O can be avoided by rotation along the N–C bond, the molecule takes a similar conformation to compounds 2–7. Because of the bulky size of the ethyl group, the dihedral angle is moderately increased to

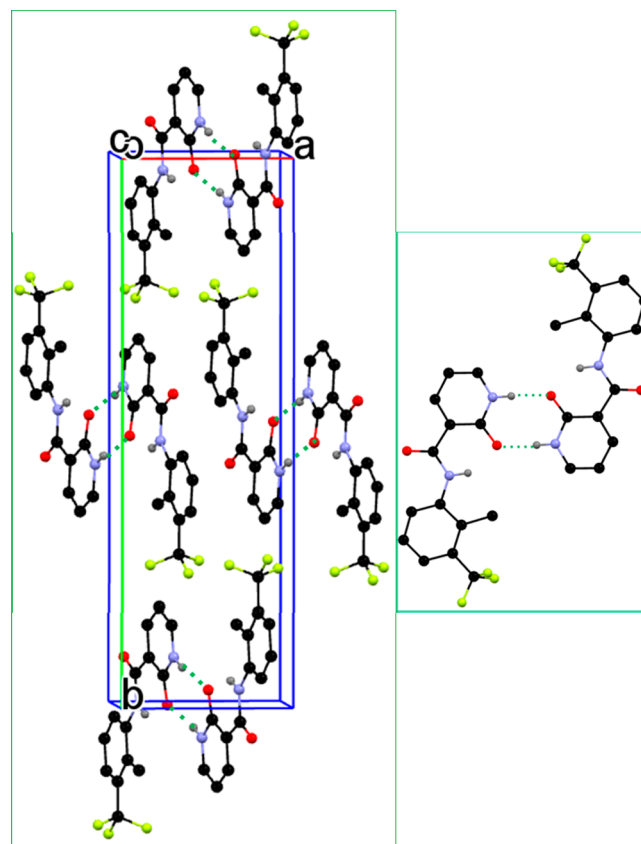


Figure 8. Crystal packing of compound 7 and the lactam–lactam synthon. For clarity, H's not participating in hydrogen bonds are omitted.

15.21(6)°. Yet, the overall hydrogen bond patterns are similar to those of compounds 1–7 (Figure 9). The hydrogen bonds parameters are as follows: 1.951 Å and 171.18° for an intermolecular hydrogen bond, and 1.949 Å and 142.96° for an intramolecular hydrogen bond.

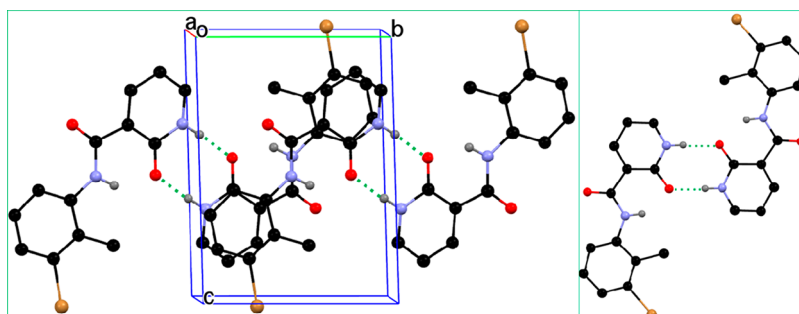


Figure 7. Crystal packing of compound 6 and the lactam–lactam synthon. For clarity, H's not participating in hydrogen bonds are omitted.

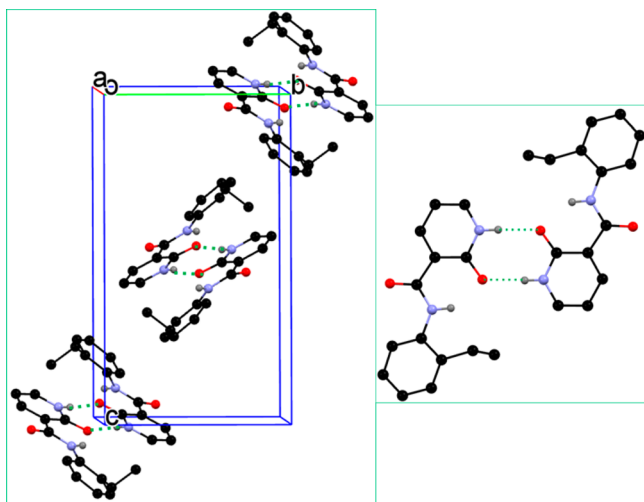


Figure 9. Crystal packing of compound **8** and the lactam–lactam synthon. For clarity, H's not participating in hydrogen bonds are omitted.

For compounds **9–12** (Figure 1), substituents such as methyl, ethyl, and isopropyl groups are installed at both ortho positions of the aniline. As a result, we can imagine the molecules no longer take (near) planar conformations since a planar conformation would lead to unavoidable steric repulsion between the amide C=O and the substituent. The molecules in compounds **9–12** crystallized in space group $P2_1/c$ as shown in the crystallographic data in Table 3. As expected, all the molecules take a twisted conformation by rotating along the N–C bond to avoid the steric effect, as suggested by the dihedral angles between the two aromatic rings (Table 4). This

Table 4. Values of the Dihedral Angle, τ , of the Molecules in the Crystal Structures of compounds **9–12**

9	10	11	12
57.67 (4)°	42.04 (5)°	77.79(9)°	56.83 (3)°

conformation change leads to a hydrogen bond pattern variation. The lactam–lactam dimer persistent in compounds **1–8** is no longer observed in compounds **9–12**, and instead a chain based on the hydrogen bond between the amide C=O and the lactam NH is formed. The amide NH only formed a hydrogen bond with the lactam C=O intramolecularly.

Compound 9. Compound **9** has two methyl groups at the ortho positions of the aniline. The molecule is twisted with the dihedral angle of 57.67 (4)° (Figure 10). The intermolecular hydrogen bond has a bond length of 1.955 Å and a bond angle of 156.21°, and the intramolecular hydrogen bond has parameters of 1.960 Å for bond length and 137.36° for bond angle.

Compound 10. Compared with compound **9**, other than two methyl groups at the ortho position of the aniline, a third methyl was introduced at the para position for compound **10**. The molecule is twisted similar to compound **9**, although to a lesser degree, with a dihedral angle of 42.04(5)° (Figure 11). The corresponding hydrogen bond parameters are as follows: intermolecular hydrogen bond: 1.927 Å and 161.59°, and intramolecular hydrogen bond: 1.949 Å and 138.45°.

Compound 11. Compound **11** has two ethyl groups at the ortho positions of the aniline. Although the size of ethyl is nearly doubled compared to that of methyl, the steric repulsion is not increased since the CH₃ of the ethyl group can point away from NH; thus, the molecule has a twisted conformation with a similar dihedral angle of 56.83(3)° (Figure 12). The

Table 3. Crystallographic Data of Compounds **9–12**

	9	10	11	12
formula	C ₁₄ H ₁₄ N ₂ O ₂	C ₁₅ H ₁₆ N ₂ O ₂	C ₁₆ H ₁₈ N ₂ O ₂	C ₁₈ H ₂₂ N ₂ O ₂
formula weight	242.27	256.30	270.32	298.38
crystal size	0.25 × 0.20 × 0.15	0.50 × 0.10 × 0.10	0.40 × 0.15 × 0.10	0.30 × 0.20 × 0.10
crystal system	monoclinic	monoclinic	monoclinic	monoclinic
space group	$P2_1/c$	$P2_1/c$	$P2_1/c$	$P2_1/c$
$a/\text{Å}$	7.679(1)	3.913(1)	8.12190(10)	9.3920(4)
$b/\text{Å}$	11.305(2)	27.948(6)	11.8718(2)	13.3660(6)
$c/\text{Å}$	14.488(2)	11.494(3)	14.1835(3)	13.4321(7)
$\alpha/^\circ$	90	90	90	90
$\beta/^\circ$	102.99(1)	99.33(1)	94.0379(7)	91.994(2)
$\gamma/^\circ$	90	90	90	90
Z, Z'	4, 1	4, 1	4, 1	4, 1
$V/\text{Å}^3$	1225.5(3)	1240.4(5)	1364.20(4)	1685.16(14)
$D_{\text{cal}}/\text{g cm}^{-3}$	1.313	1.372	1.316	1.176
T/K	90.0(2)	90.0(2)	90.0(2)	90.0(2)
Abs coeff (mm ⁻¹)	0.089	0.092	0.089	0.077
$F(000)$	512	544	576	640
θ range (deg)	2.31–27.48	1.46–27.47	2.24–27.46	2.15–27.49
limiting indices	$-9 \leq h \leq 9$ $-14 \leq k \leq 14$ $-18 \leq l \leq 18$	$-5 \leq h \leq 5$ $-36 \leq k \leq 36$ $-14 \leq l \leq 14$	$-10 \leq h \leq 10$ $-15 \leq k \leq 15$ $-18 \leq l \leq 18$	$-12 \leq h \leq 12$ $-17 \leq k \leq 17$ $-17 \leq l \leq 17$
completeness to 2θ (%)	100	99.9	99.9	99.9
unique reflections	1970	1907	2497	1778
$R_1 [I > 2\sigma(I)]$	0.0491	0.0466	0.0408	0.0694
wR_2 (all data)	0.1468	0.1355	0.1122	0.2235
CCDC accession code	1975939	1975940	1975841	1975842

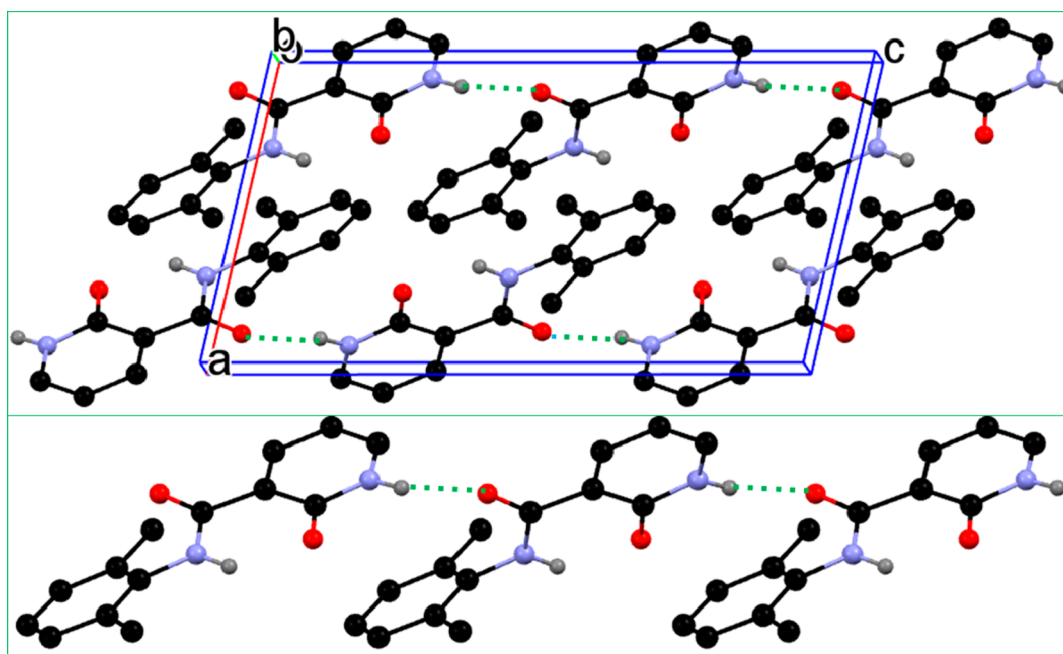


Figure 10. Crystal packing of compound **9** and the lactam–lactam synthon. For clarity, H's not participating in hydrogen bonds are omitted.

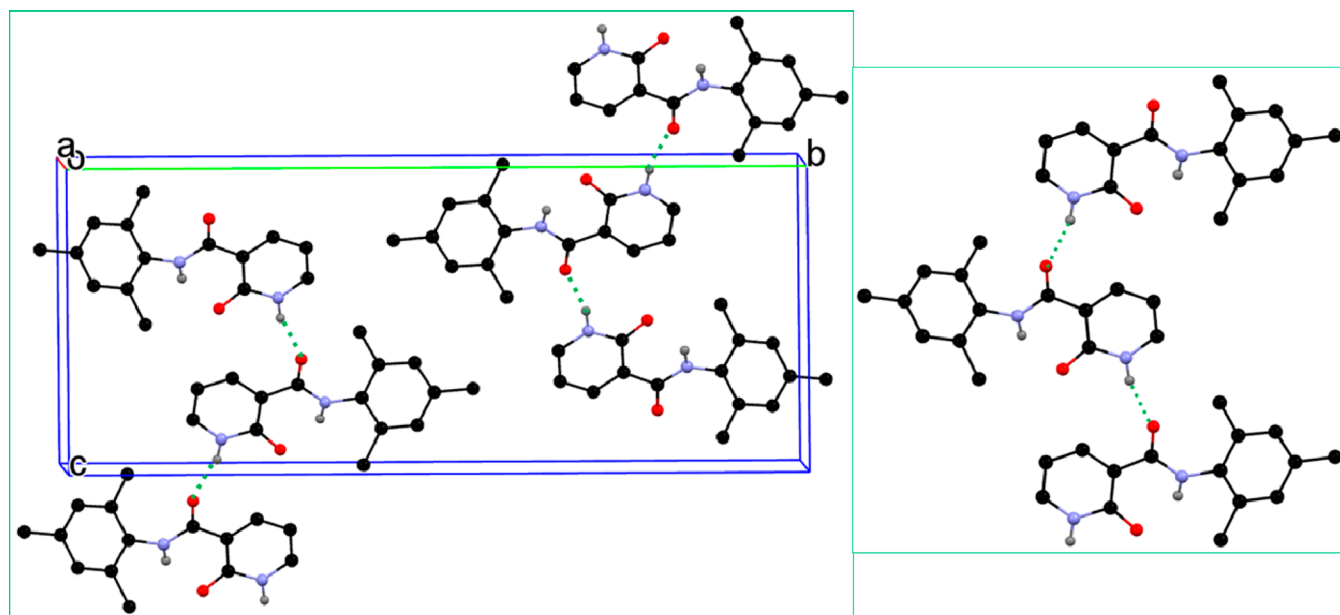


Figure 11. Crystal packing of compound **10** and the lactam–lactam synthon. For clarity, H's not participating in hydrogen bonds are omitted.

intermolecular hydrogen bond has a bond length of 1.914 Å and a bond angle of 166.05°, and the intramolecular hydrogen bond parameters are 1.935 Å for bond length, and 137.64° for bond angle.

Compound 12. The two isopropyl groups at the ortho positions of the aniline lead to a dramatic increase of steric repulsion between amide NH and CH(CH₃)₂, causing a drastic increase of the dihedral angle (77.79(9)°) (Figure 13). The corresponding hydrogen bonds have parameters of 1.871 Å and 168.44° intermolecularly, and 1.924 Å and 138.06° intramolecularly.

In a related study of substituted *N*-aryl-2-chloronicotinamides, 2-ClC₆H₃NCONHC₆H₄X-4', the hydrogen bonding motifs vary upon the substituents on the benzene ring as both

the amide NH...O=C catemer and amide NH...N_{pyridine} chain (Figure 14), and other hydrogen bonding patterns are observed.²⁶

3.2. Computation. Questions are raised after examining the dramatic structural difference between these two series of compounds: why do the molecules with negligible steric hindrance not form chain structures based either on amide NH...C=O or lactam NH...C=O (amide), like that in compounds 9–12? And why the molecules with significant steric hindrance do not form amide NH...O=C or lactam–lactam dimer? We turned to theoretical calculations for answers.

Compounds **1** and **9** (for molecules, **M1** and **M9** are used) are selected as representatives of these two series of

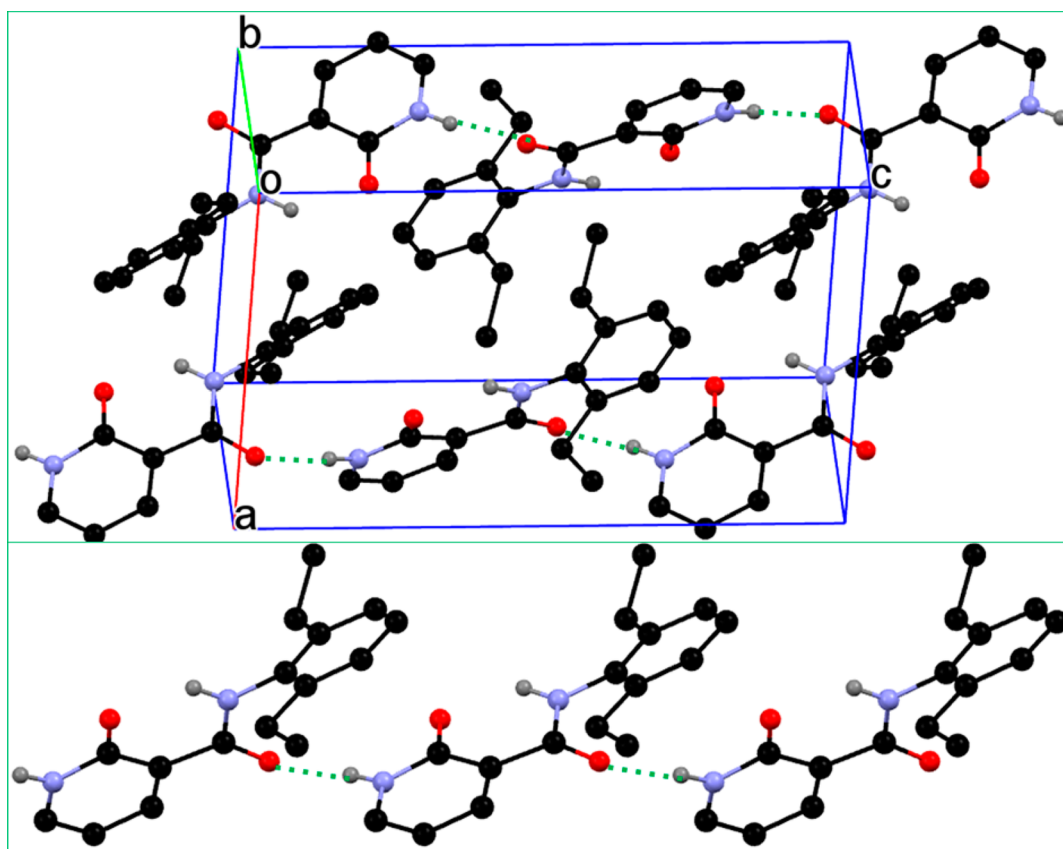


Figure 12. Crystal packing of compound 11 and the lactam–lactam synthon. For clarity, H's not participating in hydrogen bonds are omitted.

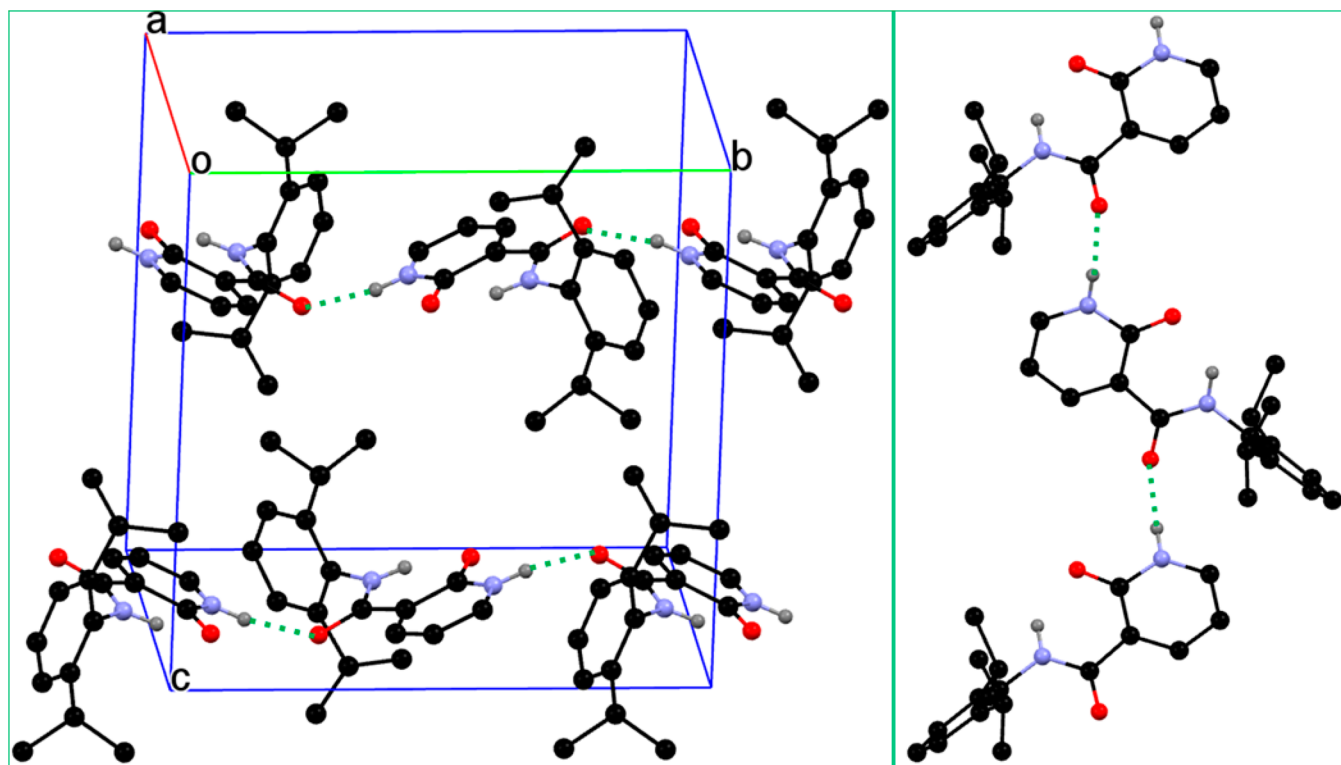


Figure 13. Crystal packing of compound 12 and the lactam–lactam synthon. For clarity, H's not participating in hydrogen bonds are omitted.

compounds. As shown in Figure 15, the most stable conformation of M1 is planar. The hydrogen atoms in the benzene and lactam rings shield the lone pair electrons on the

oxygen atom of the amide C=O by forming two $sp^2C-H\cdots O$ hydrogen bonds, preventing the molecules from forming a hydrogen bond between amide C=O and amide NH or

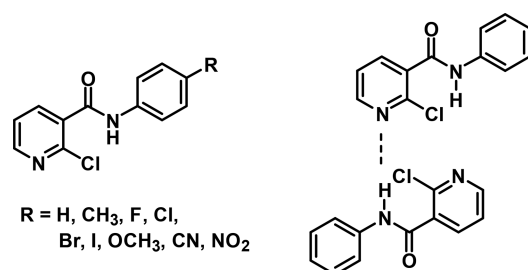


Figure 14. *N*-Aryl-2-chloronicotinamides and the observed NH...*N*_{pyridine} hydrogen bond.

lactam NH (as in compound **9**), which would mean the molecule takes a twisted conformation as does **M9** (see Figure 16), thus breaking the conjugation between the benzene ring and the amide, which makes the stabilizing energy lower. As a result, the **M1**s form lactam–lactam dimers. In contrast, **M9** is twisted with symmetrical minima (Figure 15c) due to the steric effect between the ortho methyl on the benzene ring and oxygen in the amide C=O. The amide C=O hydrogen bonds with ^{sp}²C–H of the lactam ring. Yet, the other lone pair of C=O is freed due to the twisted conformation, ready to participate in hydrogen bonding. Moreover, as shown in Figure 17, the electrostatic potential around the amide oxygen (−45.11 kcal/mol) is significantly higher than that of the lactam oxygen (−31.24 kcal/mol) in **M9**, which means the amide C=O is better matched with the lactam NH with an electrostatic potential of 54.27 kcal/mol. Therefore, **M9** molecules prefer to form hydrogen bonds between the amide C=O and lactam NH, leading to a catmer motif. The choice of hydrogen bond motifs in **M1** and **M9** is also explained by further calculations. As shown in Figure 18, the stabilizing energy, defined as $\Delta E_{\text{stabilizing}} = 1/2 (E_{\text{lactam-lactam dimer}} - 2 E_{\text{monomer}})$ for lactam–lactam dimer and $\Delta E_{\text{stabilizing}} = E_{\text{catemer}} - 2 E_{\text{monomer}}$ for catemer, was calculated. For **M9**, the two symmetrical minima are enantiomers to each other. Theoretically, there are two types of dimers, i.e., PP/MM and PM dimers. Since the lactam–lactam dimer formation is not affected by the chirality of molecule, these two dimers have almost identical energy (Table 5). All geometries were optimized in a vacuum at the B3LYP[1–2]/6-311+g(d) level by Gaussian 16.^{27–29} The solvent effects of toluene, carbon tetrachloride (CCl₄), dichloromethane (DCM), and methanol were considered by the PCM model. It is obvious that the lactam–lactam dimer is more stable than the catemer in **M1** regardless of the polarity of solvents, in contrast with the situation in **M9**. Thus, it can be deduced that **M1** and **M9** shall follow their intrinsic intermolecular interaction mode in their crystals, echoing the experimental results.

Moreover, Hirshfeld surface analyses³⁰ (see Supporting Information) confirmed that intermolecular interactions in all compounds are mainly from lactam...lactam (**1–8**) or lactam...amide (**9–12**) hydrogen bond.

4. CONCLUSION

Twelve PHNAs with various degrees of steric hindrance have been synthesized, and their crystal structures revealed their real identities to be 2-oxo-1,2-dihydropyridine-3-carboxylic acid phenylamides, their tautomers. Because of tautomerization, the molecules show a unique structural property, i.e., the coexistence of both lactam and amide functionalities, β to each other, in an end-to-end fashion. Multiple hydrogen

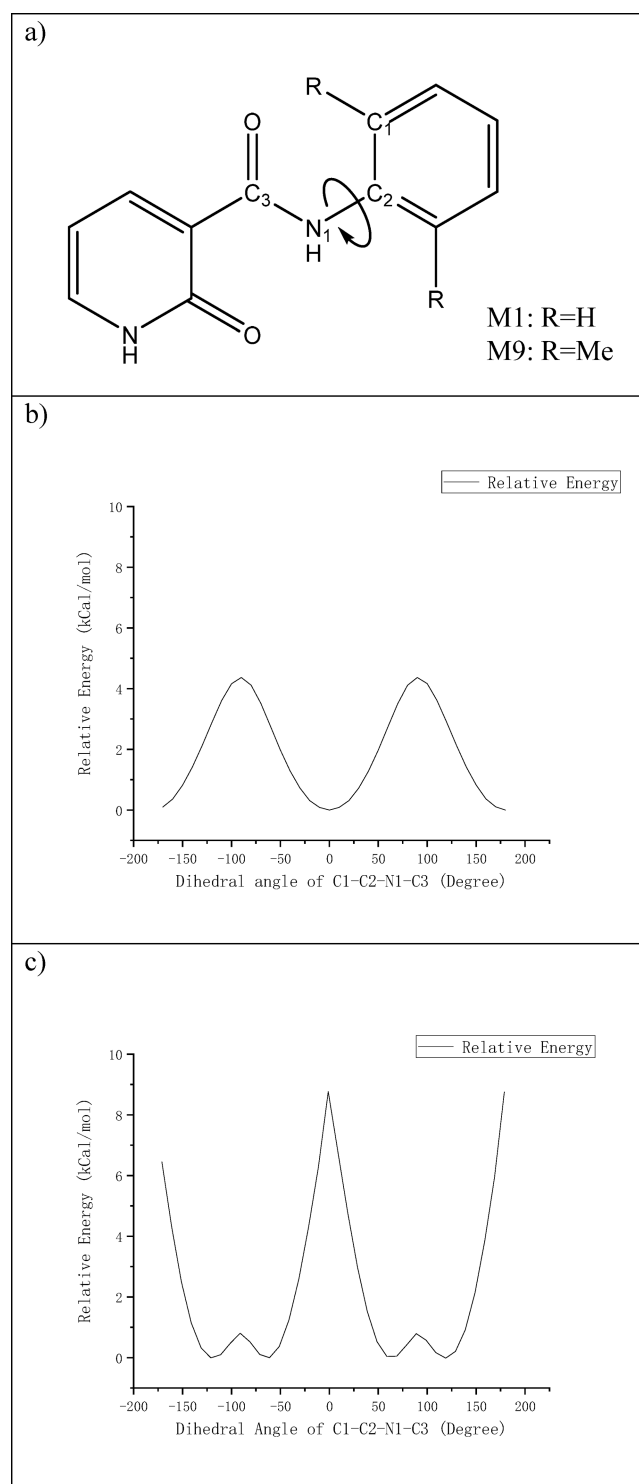


Figure 15. Correlation between relative energy (defined as $E_{\text{Relative}} = E - E_{\text{min}}$ where E_{min} is the energy of most stable conformation) and dihedral angle (shown in a) of amide in (b) **M1** and (c) **M9**.

bonding possibilities could arise. Yet, only two hydrogen bonding motifs are observed, i.e., the lactam–lactam dimer in molecules with no or marginal steric hindrance, and the amide NH...O=C (lactam) catemer in the molecules with a significant steric effect due to the presence of bulky alkyl groups at both ortho positions of the aniline ring. A conformational analysis and a molecular electrostatic potential surfaces survey provided a reasonable explanation for the

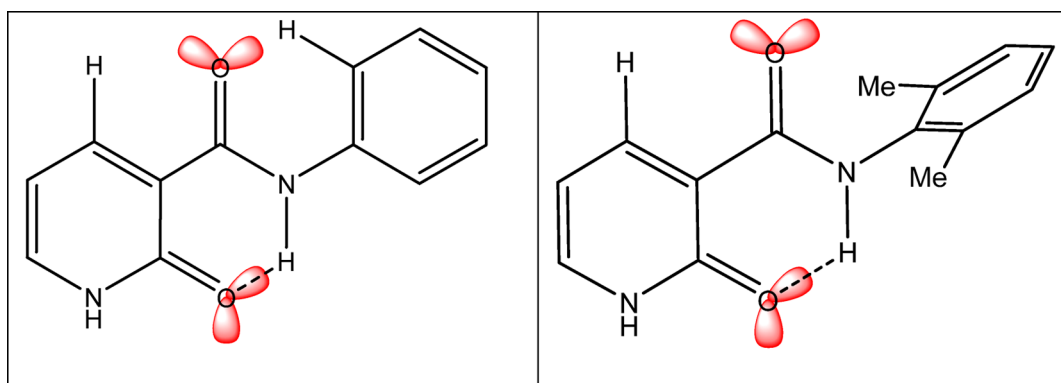


Figure 16. Sketch of lone pair electrons of (left) M1 and (right) M9.

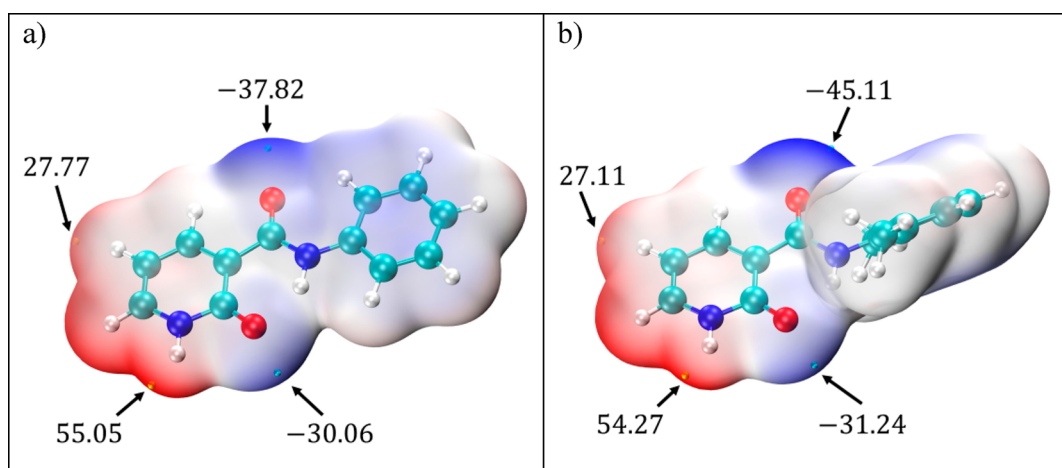


Figure 17. Electrostatic potential and local extremes on the molecular surface of (a) M1 and (b) M9 (unit: kcal/mol).

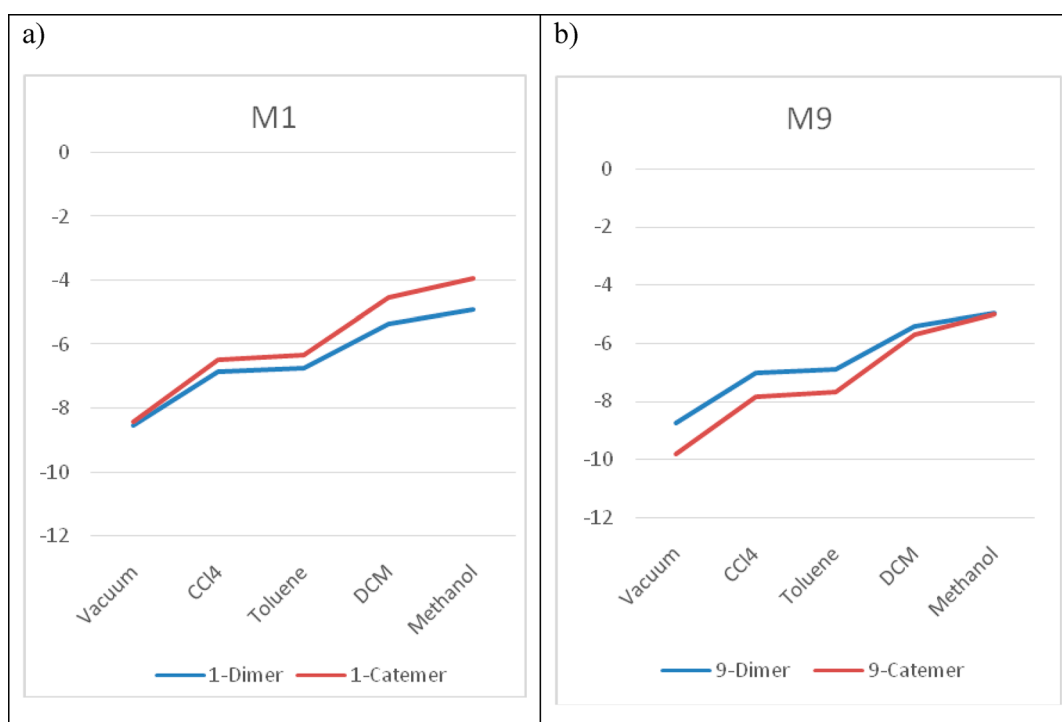
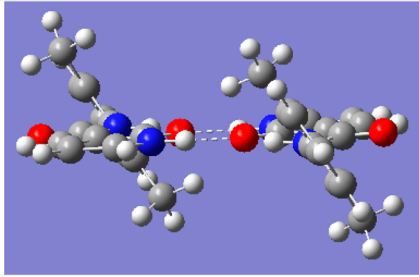
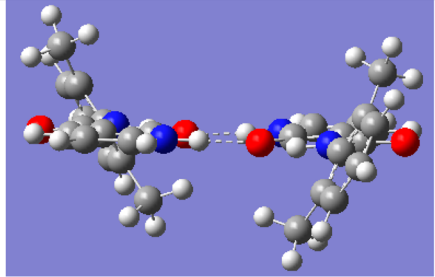


Figure 18. Stabilizing energy of (a) M1 and (b) M9.

Table 5. Relative Energy of P–M and P–P dimers

Dimer type	P-M	P-P
Point Group	C _i Point Group	C ₂ Point Group
Energies at b3lyp/6-311+g(d) level	-1604.25336044Hartree	-1604.25339309Hartree
Relative Energy	0	-0.02 kcal/mol
		

formation of these two motifs and the exclusion of other possibilities, i.e., a (near) planar molecular conformation prevents the amide NH from forming an intermolecular hydrogen bond, permitting only the formation of the lactam–lactam dimer, and while a twisted molecular conformation frees the amide NH, allowing it to participate in intermolecular hydrogen bonding with the lactam C=O due to a near perfect match of electrostatic potential surfaces. This combination of experimental and theoretical studies can be used to investigate analogues of *N*-phenyl-2-hydroxynicotinanilides such as *N*-phenyl-4-hydroxynicotinanilides and *N*-phenyl-6-hydroxynicotinanilides, which is underway. And the booming field of crystal engineering^{31–34} shall benefit from the knowledge gained in this study and to be generated from related investigations.

■ ASSOCIATED CONTENT

Supporting Information

The Supporting Information is available free of charge at <https://pubs.acs.org/doi/10.1021/acs.cgd.0c00023>.

Experimental details of synthesis and characterization of the PHNAs, crystal growth, crystal structure determination (PDF)

Accession Codes

CCDC 1975829, 1975832–1975835, and 1975838–1975842 contain the supplementary crystallographic data for this paper. These data can be obtained free of charge via www.ccdc.cam.ac.uk/data_request/cif, or by emailing data_request@ccdc.cam.ac.uk, or by contacting The Cambridge Crystallographic Data Centre, 12 Union Road, Cambridge CB2 1EZ, UK; fax: +44 1223 336033.

■ AUTHOR INFORMATION

Corresponding Authors

F. Yu – Key Laboratory for Green Chemical Process of Ministry of Education, Hubei Key Laboratory of Novel Reactor and Green Chemical Technology, Hubei Engineering Research Center for Advanced Fine Chemicals, School of Chemical Engineering and Pharmacy, Wuhan Institute of Technology, Wuhan, Hubei 430205, China; orcid.org/0000-0002-5062-8731; Phone: (027) 87194980; Email: fyuwucn@gmail.com

S. Long – Key Laboratory for Green Chemical Process of Ministry of Education, Hubei Key Laboratory of Novel Reactor and Green Chemical Technology, Hubei Engineering Research Center for Advanced Fine Chemicals, School of Chemical Engineering and Pharmacy, Wuhan Institute of Technology, Wuhan, Hubei 430205, China; orcid.org/0000-0002-4424-6374; Email: Sihuilong@wit.edu.cn, longsihui@yahoo.com

Authors

H. Liu – Key Laboratory for Green Chemical Process of Ministry of Education, Hubei Key Laboratory of Novel Reactor and Green Chemical Technology, Hubei Engineering Research Center for Advanced Fine Chemicals, School of Chemical Engineering and Pharmacy, Wuhan Institute of Technology, Wuhan, Hubei 430205, China

X. Yang – Key Laboratory for Green Chemical Process of Ministry of Education, Hubei Key Laboratory of Novel Reactor and Green Chemical Technology, Hubei Engineering Research Center for Advanced Fine Chemicals, School of Chemical Engineering and Pharmacy, Wuhan Institute of Technology, Wuhan, Hubei 430205, China

S. Cao – Key Laboratory for Green Chemical Process of Ministry of Education, Hubei Key Laboratory of Novel Reactor and Green Chemical Technology, Hubei Engineering Research Center for Advanced Fine Chemicals, School of Chemical Engineering and Pharmacy, Wuhan Institute of Technology, Wuhan, Hubei 430205, China

J. Chen – Computational Center for Molecular Science, College of Chemistry, Nankai University, Tianjin, China

M. Zhang – Computational Center for Molecular Science, College of Chemistry, Nankai University, Tianjin, China

S. Parkin – Department of Chemistry, University of Kentucky, Lexington, Kentucky 40506, United States

T. Li – Department of Industrial and Physical Pharmacy, Purdue University, West Lafayette, Indiana 47907, United States; orcid.org/0000-0003-2491-0263

Z. Yang – Key Laboratory of Biotechnology of Antibiotics, Ministry of Health, Institute of Medicinal Biotechnology, Chinese Academy of Medical Sciences & Peking Union Medical College, Beijing 100050, China

Complete contact information is available at:
<https://pubs.acs.org/10.1021/acs.cgd.0c00023>

Author Contributions

#H.L. and X.Y. contributed equally to this study.

Notes

The authors declare no competing financial interest.

ACKNOWLEDGMENTS

H.L. and S.L. thank Natural Science Foundation of Hubei Province for financial support (2014CFB787). X.Y. is grateful for the sponsorship from Innovation Fund of the Graduate School of WIT (CX2019018). Z.Y. thanks the National Natural Science Foundation of China for providing financial support (81172965 and 81321004).

REFERENCES

- (1) Huang, C.; Hsieh, Y.; Huang, W.; Lee, A. Synthesis of N-(4-Substituted Phenyl)-2-hydroxynicotinilides as Potential Anti-inflammatory Agents. *Chin. Pharm. J.* **2006**, *58*, 105–113.
- (2) Huang, C.; Hsieh, Y.; Huang, W.; Lee, A. Synthesis of N-(Chlorophenyl)-2-hydroxynicotinilides as Potential Anti-inflammatory Agents. *Chin. Pharm. J.* **2007**, *59*, 39–45.
- (3) Huang, C.; Hsieh, Y.; Huang, W.; Lee, A. Anti-inflammatory Activity and Structure-activity Relationships of N-(Substituted phenyl)-5-methylisoxazole-3-carboxamides. *Chin. Pharm. J.* **2007**, *59*, 203–210.
- (4) Long, S.; Zhou, P.; Theiss, K. L.; Siegler, M. A.; Li, T. Solid-state identity of 2-hydroxynicotinic acid and its polymorphism. *CrystEngComm* **2015**, *17*, 5195–5205.
- (5) Long, S.; Zhang, M.; Zhou, P.; Yu, F.; Parkin, S.; Li, T. Tautomeric Polymorphism of 4-Hydroxynicotinic Acid. *Cryst. Growth Des.* **2016**, *16*, 2573–2580.
- (6) Gupta, S.; Long, S.; Li, T. 6-Oxo-1, 6-dihydropyridine-3-carboxylic acid. *Acta Crystallogr., Sect. E: Struct. Rep. Online* **2007**, *63*, o2784–o2784.
- (7) Joseph, A.; Rodrigues Alves, J. S.; Bernardes, C. E. S.; Piedade, M. F. M.; Minas da Piedade, M. E. Tautomer selection through solvate formation: the case of 5-hydroxynicotinic acid. *CrystEngComm* **2019**, *21*, 2220–2233.
- (8) Rodriguez-Lucena, D.; Benito, J. M.; Mellet, C. O.; Garcia Fernandez, J. M. Promoting helicity in carbohydrate-containing foldamers through long-range hydrogen bonds. *Chem. Commun.* **2007**, *8*, 831–833.
- (9) Balamurugan, D.; Muraleedharan, K. M. Can Helical Peptides Unwind One Turn at a Time? Controlled Conformational Transitions in α , $\beta^{2,3}$ -Hybrid Peptides. *Chem. - Eur. J.* **2015**, *21*, 9332–9338.
- (10) Kovács, B.; Geudens, N.; Martins, J., Direct detection of NH...O=C H-bonds in a ¹³C- and ¹⁵N-labelled Cyclic Lipopeptide and the Investigation of its Self-Assembly. In *28th International Conference on Magnetic Resonance in Biological Systems*, 2018.
- (11) Grzesiak, A. L.; Lang, M.; Kim, K.; Matzger, A. J. Comparison of the four anhydrous polymorphs of carbamazepine and the crystal structure of form I. *J. Pharm. Sci.* **2003**, *92*, 2260–2271.
- (12) Harris, R. K.; Ghi, P. Y.; Puschmann, H.; Apperley, D. C.; Griesser, U. J.; Hammond, R. B.; Ma, C.; Roberts, K. J.; Pearce, G. J.; Yates, J. R.; Pickard, C. J. Structural studies of the polymorphs of carbamazepine, its dihydrate, and two solvates. *Org. Process Res. Dev.* **2005**, *9*, 902–910.
- (13) Babu, N. J.; Reddy, L. S.; Nangia, A. Amide- n-oxide heterosynthon and amide dimer homosynthon in cocrystals of carboxamide drugs and pyridine n-oxides. *Mol. Pharmaceutics* **2007**, *4*, 417–434.
- (14) Long, S.; Siegler, M.; Li, T. N-(3-Chloro-2-methylphenyl)-2-oxo-1, 2-dihydropyridine-3-carboxamide. *Acta Crystallogr., Sect. E: Struct. Rep. Online* **2006**, *62*, o4278–o4279.
- (15) Liu, S.; Zhu, S.; Wu, Y.; Gao, J.; Qian, P.; Hu, Y.; Shi, L.; Chen, S.; Zhang, S.; Zhang, Y. One-Pot Synthesis of N-Aryl-Nicotinamides and Diarylamines Based on a Tunable Smiles Rearrangement. *Eur. J. Org. Chem.* **2015**, *2015*, 3048–3052.
- (16) Liu, H.; Yang, X.; Wu, S.; Zhang, M.; Parkin, S.; Cao, S.; Li, T.; Yu, F.; Long, S. An investigation of the polymorphism of a potent nonsteroidal anti-inflammatory drug flunixin. *CrystEngComm* **2020**, *22*, 448–457.
- (17) *Collect*; Nonius BV: Delft, the Netherlands, 2002.
- (18) Otwinowski, Z.; Minor, W. I. *Methods in Enzymology: Macromolecular Crystallography, Part A*; Carter, C. W., Jr., Sweet, R. M., Eds.; Academic Press: New York, 1997; pp 276, 307–326.
- (19) Sheldrick, G. M. SHELXL-97: Program for the Refinement of Crystal Structures; University of Gottingen, 1997.
- (20) Sheldrick, G. M. A short history of SHELX. *Acta Crystallogr., Sect. A: Found. Crystallogr.* **2008**, *64*, 112–122.
- (21) Kaseyama, T.; Furumi, S.; Zhang, X.; Tanaka, K.; Takeuchi, M. Hierarchical assembly of a phthalhydrazide-functionalized helicene. *Angew. Chem., Int. Ed.* **2011**, *50*, 3684–3687.
- (22) Long, S.; Li, T. Enforcing molecule's π -conjugation and consequent formation of the acid- acid homosynthon over the acid-pyridine heterosynthon in 2-anilinicotinic acids. *Cryst. Growth Des.* **2010**, *10*, 2465–2469.
- (23) Lima, L. M.; Barreiro, E. J. Bioisosterism: a useful strategy for molecular modification and drug design. *Curr. Med. Chem.* **2005**, *12*, 23–49.
- (24) Jeschke, P. The unique role of halogen substituents in the design of modern crop protection compounds. *Mod. Methods Crop Prot. Res.* **2013**, 73–128.
- (25) Jeffries, B.; Wang, Z.; Graton, J.; Holland, S. D.; Brind, T.; Greenwood, R. D.; Le Questel, J. Y.; Scott, J. S.; Chiarparin, E.; Linclau, B. Reducing the Lipophilicity of Perfluoroalkyl Groups by CF₂-F/CF₂-Me or CF₃/CH₃ Exchange. *J. Med. Chem.* **2018**, *61*, 10602–10618.
- (26) Cuffini, S.; Glidewell, C.; Low, J. N.; De Oliveira, A. G.; De Souza, M. V.; Vasconcelos, T. R.; Wardell, S. M.; Wardell, J. L. Nine N-aryl-2-chloronicotinamides: supramolecular structures in one, two and three dimensions. *Acta Crystallogr., Sect. B: Struct. Sci.* **2006**, *62*, 651–665.
- (27) Frisch, M.; Trucks, G.; Schlegel, H.; Scuseria, G.; Robb, M.; Cheeseman, J.; Scalmani, G.; Barone, V.; Petersson, G.; Nakatsuji, H. *J. I. Gaussian 16*, Revision A.03; Gaussian, Wallingford, CT, 2016.
- (28) Stephens, P. J.; Devlin, F.; Chabalowski, C.; Frisch, M. J. Ab initio calculation of vibrational absorption and circular dichroism spectra using density functional force fields. *J. Phys. Chem.* **1994**, *98*, 11623–11627.
- (29) Becke, A. D. Density-functional thermochemistry. III. The role of exact exchange. *J. Chem. Phys.* **1993**, *98*, 5648–5652.
- (30) Spackman, M. A.; Jayatilaka, D. Hirshfeld Surface Analysis. *CrystEngComm* **2009**, *11*, 19–32.
- (31) Pepinsky, R. Crystal engineering-new concept in crystallography. *Phys. Rev.* **1955**, *100*, 971.
- (32) Schmidt, G. M. J. Photodimerization in the solid state. *Pure Appl. Chem.* **1971**, *27*, 647–678.
- (33) Corpinot, M. K.; Bučar, D. K. A Practical Guide to the Design of Molecular Crystals. *Cryst. Growth Des.* **2019**, *19*, 1426–1453.
- (34) Nangia, A. K.; Desiraju, G. R. Crystal Engineering: An Outlook for the Future. *Angew. Chem., Int. Ed.* **2019**, *58*, 4100–4107.